

## Orbital Dynamics and the Evolution of Planetary Habitability in the AU Mic System

STEPHEN R. KANE,<sup>1</sup> BRADFORD J. FOLEY,<sup>2</sup> MICHELLE L. HILL,<sup>1</sup> CAYMAN T. UNTERBORN,<sup>3</sup> THOMAS BARCLAY,<sup>4,5</sup>  
BRYSON CALE,<sup>6</sup> EMILY A. GILBERT,<sup>7,8,9,5,10</sup> PETER PLAVCHAN,<sup>6</sup> AND JUSTIN M. WITTRICK<sup>6</sup>

<sup>1</sup>*Department of Earth and Planetary Sciences, University of California, Riverside, CA 92521, USA*

<sup>2</sup>*Department of Geosciences, Pennsylvania State University, University Park, PA 16802, USA*

<sup>3</sup>*Southwest Research Institute, San Antonio, TX 78238, USA*

<sup>4</sup>*University of Maryland, Baltimore, MD 21250, USA*

<sup>5</sup>*NASA Goddard Space Flight Center, Greenbelt, MD 20771, USA*

<sup>6</sup>*Department of Physics & Astronomy, George Mason University, Fairfax, VA 22030, USA*

<sup>7</sup>*Department of Astronomy and Astrophysics, University of Chicago, Chicago, IL 60637, USA*

<sup>8</sup>*University of Maryland, Baltimore County, Baltimore, MD 21250, USA*

<sup>9</sup>*The Adler Planetarium, Chicago, IL 60605, USA*

<sup>10</sup>*GSFC Sellers Exoplanet Environments Collaboration*

### ABSTRACT

The diversity of planetary systems that have been discovered are revealing the plethora of possible architectures, providing insights into planet formation and evolution. They also increase our understanding of system parameters that may affect planetary habitability, and how such conditions are influenced by initial conditions. The AU Mic system is unique among known planetary systems in that it is a nearby, young, multi-planet transiting system. Such a young and well characterized system provides an opportunity to study orbital dynamical and habitability studies for planets in the very early stages of their evolution. Here, we calculate the evolution of the Habitable Zone of the system through time, including the pre-main sequence phase that the system currently resides in. We discuss the planetary atmospheric processes occurring for an Earth-mass planet during this transitional period, and provide calculations of the climate state convergence age for both volatile rich and poor initial conditions. We present results of an orbital dynamical analysis of the AU Mic system that demonstrate the rapid eccentricity evolution of the known planets, and show that terrestrial planets within the Habitable Zone of the system can retain long-term stability. Finally, we discuss follow-up observation prospects, detectability of possible Habitable Zone planets, and how the AU Mic system may be used as a template for studies of planetary habitability evolution.

*Keywords:* astrobiology – planetary systems – planets and satellites: dynamical evolution and stability  
– stars: individual (AU Microscopii)

### 1. INTRODUCTION

The evolution of surface conditions on terrestrial planets has numerous driving factors, including the orbital dynamics within the system and the impact of the host star and planetary interior on the atmosphere (Kasting & Catling 2003; Lammer et al. 2009). These particular factors can undergo dramatic changes during the early history of the planetary system as the star moves through a period of early evolution and activity (Baraffe et al. 2002), the planets inter-

act with each other and remaining formation material (Raymond et al. 2012), and the planetary interiors contribute to the atmospheric inventory via degassing (Gaillard & Scaillet 2014). Discoveries of young planetary systems thus provide insight into the conditions present during this rapidly changing period of planetary system evolution, especially those systems that are relatively nearby. Examples of nearby young (< 50 Myrs) systems with transiting planets include V1298 Tau (David et al. 2019b,a), located at a distance of ~108 pcs, and DS Tuc (Newton et al. 2019), located at a distance of ~44 pcs. These systems provide excellent opportunities for follow-up observations, such as direct imaging observations that could extract

further properties of the young planets (Davies 1980; Kane et al. 2018).

One of the closest young planetary systems currently known is the case of AU Microscopii (hereafter AU Mic). The star is located at a distance of only 9.79 pcs, has an age estimate of  $\sim 22$  Myrs (Mamajek & Bell 2014), is a famous flare star (Plavchan et al. 2020), and is well known to harbor a substantial debris disk (Strubbe & Chiang (2006); MacGregor et al. (2013)). A planet orbiting the star was discovered by Plavchan et al. (2020) using photometry from the Transiting Exoplanet Survey Satellite (TESS; Ricker et al. (2015)) and radial velocities (RV) acquired using the iSHELL (Cale et al. 2019), HARPS (Pepe et al. 2000), and HIRES (Vogt et al. 1994) instruments. The planet has a radius of  $0.4 R_J$ , a mass of  $0.18 M_J$ , and an orbital period of 8.46 days. An additional planet was detected in an orbital period of 18.86 days by Cale et al. (2021) via further transit and RV observations. The relative youth of this system serves as a laboratory for exploring the early dynamical stability of orbits, and can inform the viability of planetary orbits in an evolving Habitable Zone (HZ).

In this paper, we present the results of a dynamical analysis of the AU Mic system, and a study of the HZ evolution and potential planets within that region. This system is not only young, but nearby, and is therefore an excellent target for numerous observational follow-up studies in addition to those that have been carried out. In particular, the prospect of eventual terrestrial planet detections at stable orbital locations would serve as a benchmark for providing a data-driven evaluation of concepts regarding early terrestrial planet formation and the evolution of their atmospheres. Section 2 describes the system properties and the extent of the HZ at the present epoch. In Section 3 we provide calculations of the HZ evolution through time based on stellar isochrones for the host star, and discuss planetary degassing models during the short-term and long-term history of the system using various initial condition assumptions. Section 4 provides the results of a dynamical analysis of the known planets, and a detailed study of possible viable orbits for terrestrial planets at farther distances, including locations within the HZ. In Section 5 we discuss the implications of the system evolution and opportunities for follow-up observations and studies, and provide concluding remarks.

## 2. SYSTEM PROPERTIES AND HABITABLE ZONE

As one of the youngest known exoplanet hosts, the properties of the host star have been the sub-

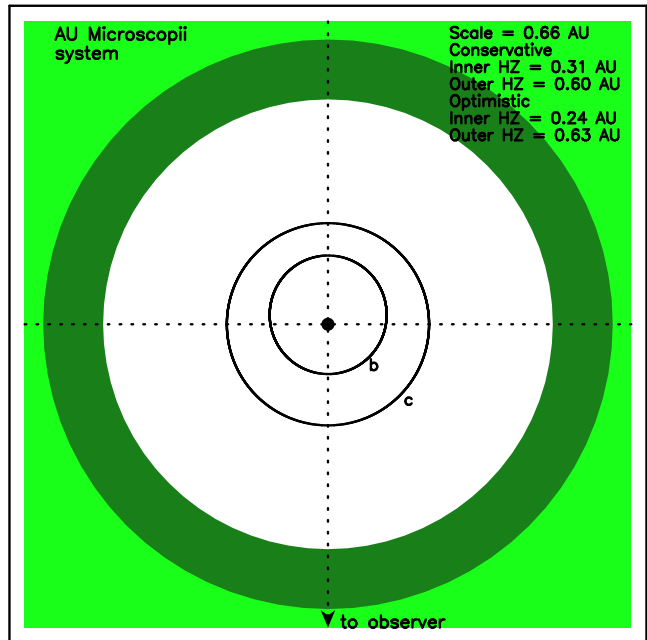


**Figure 1.** A top-down view of the AU Mic system with respect to the HZ. The star is located at the center of the crosshairs and the orbits of the known planets are shown. The CHZ and OHZ are indicated by the light green and dark green regions, respectively.

ject of numerous studies (e.g., Mamajek & Bell 2014; Kochukhov & Reiners 2020). We adopt the stellar properties provided by Plavchan et al. (2020), including the stellar effective temperature of  $T_{\text{eff}} = 3700$  K, luminosity of  $L_{\star} = 0.09 L_{\odot}$ , and mass of  $M_{\star} = 0.5 M_{\odot}$ . Note that the luminosity is relatively high due to the pre-main sequence evolutionary stage of the star, discussed in more detail in Section 3. The system is known to contain two planets, b and c, described in detail by Cale et al. (2021). Planet b has an orbital period of  $P_b = 8.46$  days, semi-major axis of  $a_b = 0.0645$  AU, eccentricity of  $e_b = 0.186$ , and planet mass of  $M_{p,b} = 20.12 M_{\oplus}$ . Planet c has an orbital period of  $P_c = 18.86$  days, semi-major axis of  $a_c = 0.1101$  AU, planet mass of  $M_{p,c} = 9.60 M_{\oplus}$ , and a circular orbit is assumed.

Using the above described stellar properties, we calculate the extent of the HZ at the present epoch (Kasting et al. 1993; Kane & Gelino 2012; Kopparapu 2013; Kopparapu et al. 2014). Specifically, we adopt the conservative HZ (CHZ) boundaries, defined by the runaway and maximum greenhouse limits, and the optimistic HZ (OHZ) boundaries, defined by empirically derived estimates of when Venus and Mars may have had surface liquid water (Kasting et al. 1993; Kane et al. 2016). By adopting these HZ definitions, we calculated the extent of the CHZ and OHZ regions to be 0.31–0.60 AU and 0.24–0.63 AU, respectively. A top-down

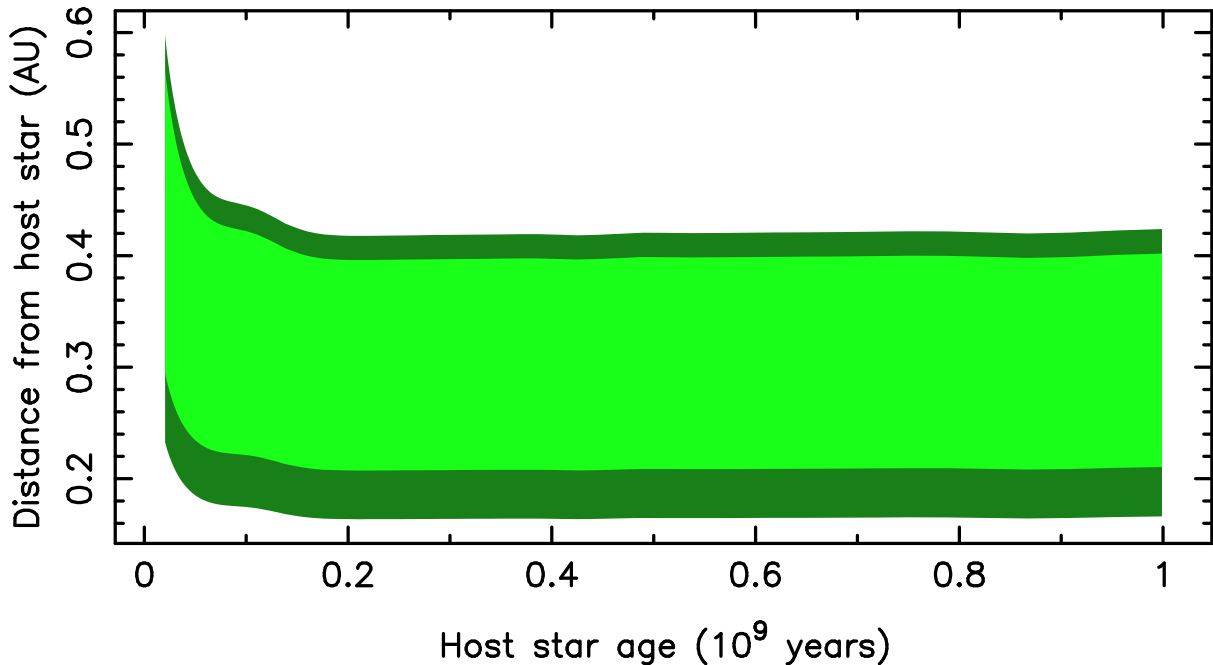


**Figure 2.** The evolving HZ for AU Mic, from the present epoch up to an age of 1 Gyr. As per Figure 1, the CHZ and OHZ are represented by the light and dark green regions, respectively. The HZ regions rapidly contract toward the star during the pre-main sequence phase, then start to gradually move away from the star after  $\sim 200$  Myrs.

view of the system, including the orbits of the known planets, is shown in Figure 1. The star is located at the center of the crosshairs, and the CHZ and OHZ are represented by the light green and dark green regions, respectively. Note that the HZ boundaries are highly dependent on stellar parameter uncertainties (Kane 2014) and distance estimate (Kane 2018). As described above, the star is both nearby and substantially characterized, and so the present HZ boundaries are likewise well defined. However, the star is also young and rapidly evolving, and so the HZ boundaries are yet to arrive at the locations that will dominate their main sequence lifetime.

### 3. PLANETARY HABITABILITY EVOLUTION

#### 3.1. *The Evolving Habitable Zone*

The evolution of stars on the main sequence, particularly with regards to their luminosity and effective temperature, results in a subsequent evolution of the HZ (Underwood et al. 2003; Ramirez & Kaltenegger 2014). This HZ evolution has been studied within the context of stellar masses and chemical compositions (Young et al. 2012; Valle et al. 2014; Truitt et al. 2015; Truitt & Young 2017), and also with respect to stellar rotation and magnetic activity (Gallet et al. 2017). The AU Mic system provides an opportunity to study the evolution of a planetary system within the context of the early luminosity environment of the host star as it

joins the main sequence. In particular, the stellar parameters adopted in Section 2 and used to calculate the HZ represent a period of rapid luminosity evolution.

To investigate the effects of the AU Mic stellar evolution on the extent of the HZ, we utilize the MESA Isochrones & Stellar Tracks (MIST) to calculate the evolutionary track (Paxton et al. 2011, 2013, 2015; Choi et al. 2016; Dotter 2016; Paxton et al. 2018, 2019). Metallicity measurements for AU Mic have produced a variety of values, ranging from  $-0.12$  dex (Gaidos et al. 2014) to  $+0.32$  dex (Neves et al. 2013). We adopt the lower metallicity values, and assume a metallicity of  $-0.1$  dex in the calculation of the evolutionary track. We further adopt the stellar mass of  $0.5 M_{\odot}$  (see Section 2) and an initial rotation rate of  $v/v_{crit} = 0.0$ . This produced stellar properties of  $T_{\text{eff}} = 3712$  K and  $L_{\star} = 0.082 L_{\odot}$  at an age of 20 Myrs; consistent with the stellar properties described in Section 2.

Figure 2 shows the evolution of the CHZ and OHZ from the present epoch up to an age of 1 Gyr. The initial HZ boundaries at an age of 20 Myrs are consistent with those shown in Figure 1, as expected. The boundaries rapidly shift inward as the star transitions to the main sequence, reaching their minimum values at  $\sim 200$  Myrs, then gradually increase with time. The period up to 200 Myrs are a particularly important era for the evolution of terrestrial planets during which the secondary atmosphere of the planet is degassed from the

interior (Lammer et al. 2008), a process that continues well into the stellar main sequence phase. Furthermore, the presence of two known giant planets interior to the HZ presents an architecture that may have significant consequences for terrestrial planets in the HZ. Several dynamical studies have shown that the formation and migration of giant planets through the HZ does not necessarily eliminate the presence of terrestrial planets in that region, and in fact may promote terrestrial planet formation in the turbulent wake of giant planet migration (Raymond et al. 2005, 2006; Fogg & Nelson 2009; Bond et al. 2010). The location of giant planets also affects the delivery of volatiles to terrestrial planets and therefore plays a major role in their surface water inventory (Raymond et al. 2004; O’Brien et al. 2018). Although a dearth of water is likely to truncate surface habitability, an over-abundance of water can also directly impede carbonate-silicate cycles and other processes required for moderating surface environments (see Section 3.2). Subsequently, the presence of terrestrial planets within these evolving HZ regions may provide critical clues regarding the early processes that can determine the eventual pathway of potentially habitable surface environments.

### 3.2. Early Terrestrial Planetary Atmospheres

Young systems, such as AU Mic, provide potential opportunities to explore the evolution of the infant stages of planetary atmospheres. These early stages can play a critical role in determining the evolutionary pathway that the planetary atmosphere will follow. For example, the planetary interior, combined with host star interaction and planetesimal impacts, will drive secondary atmosphere production and composition (Schlichting et al. 2015; Kane et al. 2020b; Kite & Barnett 2020; Oosterloo et al. 2021). The activity of the host star, particular at young ages, is a major contributor to atmospheric mass-loss, that both erodes the primary atmosphere and shapes the evolution of the secondary atmosphere (Zendejas et al. 2010; Lalitha et al. 2018; Howe et al. 2020). Moreover, atmospheric mass-loss during the early stages of planetary evolution can have a major impact on the subsequent volatile content of the atmosphere and surface (Dong et al. 2017; Roettenbacher & Kane 2017), which in turn will influence the overall habitability of the planetary surface (Luger & Barnes 2015; Dong et al. 2018; Johnstone et al. 2019). AU Mic is a particularly active star, and has significant variability including significant spot modulation and frequent white-light flares, both visible in TESS optical photometry (Gilbert et al. 2021). AU Mic flares span the full

electromagnetic spectrum ranging from x-ray to radio (Leto et al. 2000; Magee et al. 2003), including EUV flares (Tsikoudi & Kellett 2000), which are known to cause photodissociation in planetary atmospheres.

During subsequent geologic evolution, the early-formed atmosphere can be largely overprinted by continued degassing, weathering, or loss to space. As a result, it can be difficult to reconstruct the early atmospheric state of a terrestrial planet, and learn about the processes that shaped atmospheric evolution during this time. Young systems, such as AU Mic, are therefore the best opportunity to study this important time period in a planet’s history. One particularly uncertain aspect of early terrestrial planet atmospheres is whether the volatiles the planet acquires during formation (especially H & C) will mostly be outgassed to the atmosphere during, or just after, the formation process, or remain in the interior. For HZ planets with liquid surface water, subsequent weathering processes drive atmospheric CO<sub>2</sub> concentration, and hence climate, to a state dictated by the balance between the CO<sub>2</sub> outgassing and silicate weathering rates (e.g. Walker et al. 1981; Berner et al. 1983; Berner & Caldeira 1997); at this point the initial atmospheric composition, at least for CO<sub>2</sub>, is lost (e.g. Driscoll & Bercovici 2013; Foley 2015, 2019). However, it can take up to  $\sim 1$  Gyr for the initial atmospheric state to be lost due to later degassing and weathering (e.g. Driscoll & Bercovici 2013; Foley 2015, 2019). Therefore, a planet sitting in the HZ in a system like AU Mic, that is  $\sim 10$ s of Myrs old, would likely still have an atmosphere in transition from its initial state, unless atmospheric escape, or any other loss process, is fast enough to remove an atmosphere outgassed during accretion or the magma ocean phase in less than  $\sim 10$  Myrs.

To expand on the timescale for a terrestrial planet’s initial atmospheric state to be overprinted by weathering and outgassing, we use a coupled model of the carbonate-silicate cycle and interior thermal evolution. According to our calculation of the HZ for AU Mic, there is a range of orbital distances between  $\approx 0.3 - 0.4$  AU where a planet would remain in the HZ throughout the star’s evolution, including during the pre-main sequence phase. We therefore assume the planets in our models are always in the HZ and have liquid water present on their surfaces. The models further assume an Earth-like water inventory. Planets with moderately higher water inventories, such that oceans cover the surface to depths of  $\sim 10$  km or less, can likely still support a carbonate-silicate cycle (e.g. Abbot et al. 2012; Hayworth & Foley 2020). However, planets with much larger water inventories may form high pressure ice layers that prevent silicate weathering (Levi et al. 2017; Glaser et al. 2020;

Krissansen-Totton et al. 2021). We also neglect atmospheric loss in our main set of models, but explore how atmospheric loss would change our results in Section 3.3.

We calculate how long it takes for hypothetical terrestrial planets to reach approximately the same climate state when started from an initially hot, CO<sub>2</sub>-rich atmosphere versus an initially cold, CO<sub>2</sub>-poor atmosphere. The model is from Foley (2019), and calculates rates of CO<sub>2</sub> outgassing, weathering, and atmospheric CO<sub>2</sub> concentrations for rocky planets in a stagnant-lid regime, as the typical regime of tectonics for rocky planets is unknown and difficult to predict (e.g. Valencia et al. 2007; O’Neill & Lenardic 2007; Korenaga 2010; van Heck & Tackley 2011; Foley et al. 2012; Lenardic & Crowley 2012; Noack & Breuer 2014). The model calculates the rate of both volcanic degassing of mantle C and metamorphic degassing of crustal C, that is released as crust is buried to high temperature-pressure conditions. The model assumes seafloor weathering is the dominant weathering process, as forming large subaerial continents may be less likely on stagnant-lid planets. The seafloor weathering formulation is after Krissansen-Totton & Catling (2017).

We ran a set of 10<sup>4</sup> models for an Earth-like planet (same mass and core-mass fraction as Earth), randomly sampling from uncertainty ranges of the following key model parameters: the mantle reference viscosity,  $\mu_{\text{ref}}$ , which is the mantle viscosity at Earth’s present day mantle potential temperature of 1350°C; the initial mantle potential temperature,  $T_{\text{init}}$ ; the initial radiogenic heat production rate in the mantle,  $Q_0$ ; the total budget of CO<sub>2</sub> in the mantle and surface reservoirs,  $C_{\text{tot}}$ ; the reference seafloor weathering rate,  $F_{\text{sfw}}^*$ , which is defined as Earth’s estimated present day value; the activation energy for seafloor weathering,  $E_{\text{sfw}}$ ; and the exponent governing the dependence of the seafloor weathering rate on the rate of extrusive volcanism,  $\beta$ . For each model we randomly draw values of the above parameters from uniform distributions, then run one model where all of the planet’s CO<sub>2</sub> initially resides in the atmosphere, and one where the initial surface temperature is set to 273 K, such that most of the CO<sub>2</sub> initially resides in the mantle. The amount of CO<sub>2</sub> that resides in the mantle initially is a complex function of the planet’s initial bulk C budget and the pressure, temperature, and oxygen fugacity of equilibration during the formation of the central Fe-core (Kane et al. 2020a, and references therein). We then calculate how long it takes for these climate states to converge, in terms of the total planet age after system birth (the convergence age), and the time elapsed after degassing first begins (the convergence time). Stellar irradiation is assumed to be the same as what the mod-

ern Earth receives, and is held fixed in the models. The effect of varying stellar irradiation is discussed below.

We find that the mantle reference viscosity and the initial heat production rate have the biggest influence on both the climate convergence time and age (Figures 3 & 4). The reason for this is that the ability to quickly outgas CO<sub>2</sub> from the mantle is the primary control on how long it takes the two different initial climate states to converge. Silicate weathering can adjust to balance the degassing rate in  $\sim 10^5 - 10^6$  years (Berner & Caldeira 1997), so a planet starting with an initially hot, CO<sub>2</sub>-rich climate rapidly reaches a state where weathering and degassing are approximately in balance. However, degassing is much slower, so a much longer time is needed for a planet starting from an initially cold, CO<sub>2</sub>-poor atmosphere to warm up. The climate convergence time and age are therefore both primarily controlled by how quickly degassing can build up CO<sub>2</sub> on a planet where the atmosphere is initially CO<sub>2</sub>-poor. High rates of heat production and low reference viscosities favor vigorous mantle convection and rapid early outgassing, and hence lead to low convergence times and ages (Figures 3A-B & 4A-B). There is also a peak in convergence time and age at  $Q_0 \approx 70$  TW. Decreasing initial heat production rate even further leads to many planets where outgassing never occurs, as the interiors never became hot enough to melt. Such planets are not plotted here, as initial atmospheric states can not be erased by the carbonate-silicate cycle on such planets when there is no interior outgassing. The only planets able to outgas with low  $Q_0 < \approx 70$  TW are those with low reference viscosities and hence more vigorous convection.

The parameters governing seafloor weathering and the total CO<sub>2</sub> budget have a much smaller effect (Figures 3D-G & 4D-G). Both climate convergence times and ages are largely insensitive to these parameters, other than a slight dependence of the convergence time on  $C_{\text{tot}}$ . These results are consistent with the argument above that the primary factor controlling climate convergence is degassing from the interior. Silicate weathering always acts faster than degassing, so varying the parameters for silicate weathering has little effect on climate convergence. The time when climate states converge after degassing starts weakly declines with increasing  $C_{\text{tot}}$ , as more carbon in the system leads to higher degassing rates, and hence a faster convergence of the initially cold climate to the initially hot climate state.

Generally the same trends are seen when looking at either the time when climate states converge after degassing has begun, or the planet age when climate states converge. The convergence ages are higher, reaching

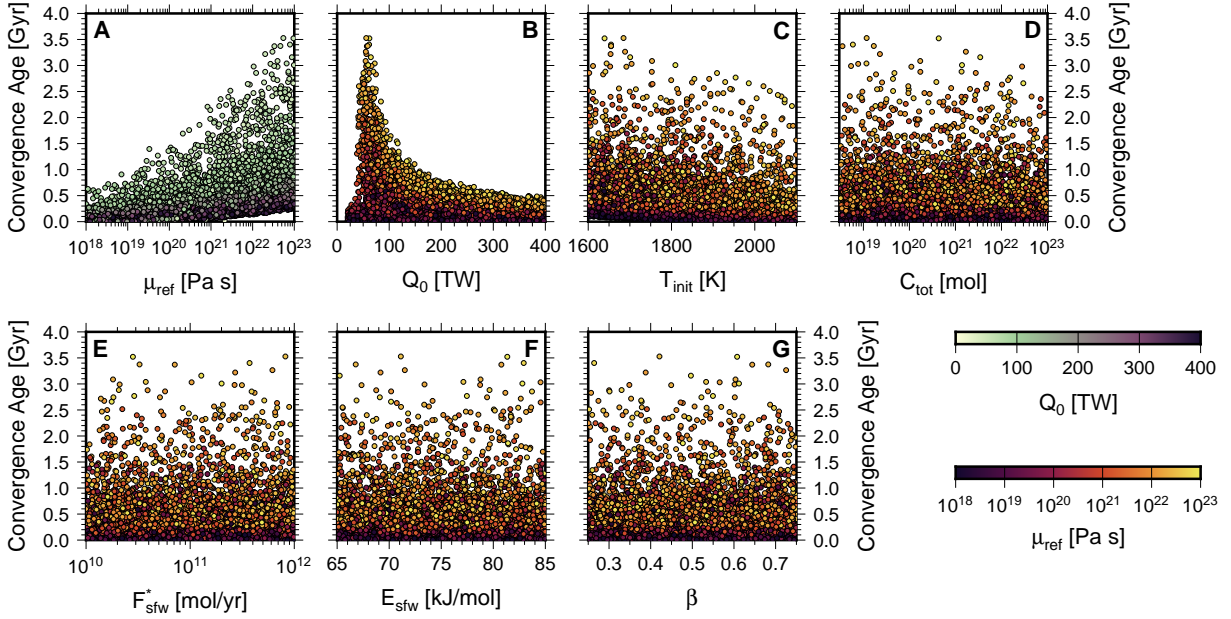


**Figure 3.** Planet age, measured after system formation, when an initially hot, CO<sub>2</sub>-rich climate and initially cold, CO<sub>2</sub>-poor climate states converge due to the negative feedbacks of the carbonate-silicate cycle. Convergence age is shown as a function of mantle reference viscosity (A), initial radiogenic heat production rate in the mantle (B), initial mantle potential temperature (C), total carbon budget of the mantle and surface reservoirs (D), reference seafloor weathering rate (E), activation energy for seafloor weathering (F), and dependence parameter of seafloor weathering on extrusive volcanism rate (G). Each symbol plotted represents one pair of model runs. Symbols are colored either by mantle reference viscosity or initial heat production rate, as denoted by the colorbars.

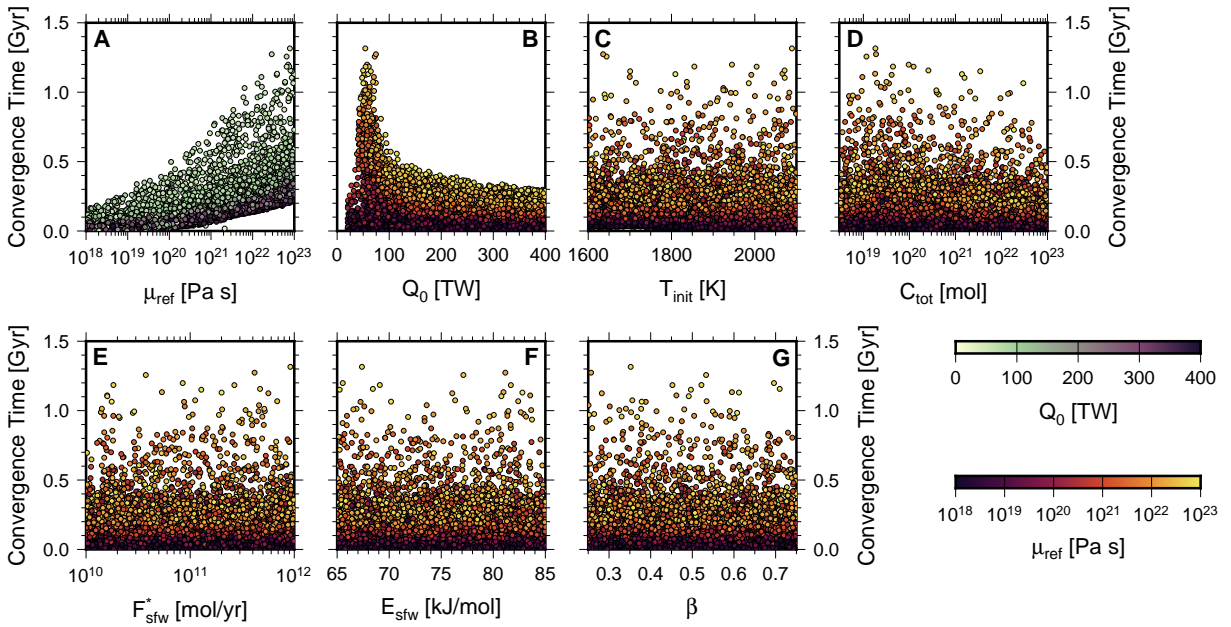


**Figure 4.** Same as Figure 3, except climate convergence is measured as the time elapsed after volcanism and degassing has begun.

$\approx 3.5\text{--}4$  Gyrs, while convergence times only reach  $\approx 1.3\text{--}1.4$  Gyrs. It can take upwards of 2–2.5 Gyrs for degassing to begin in some cases, leading to this difference. In particular, the same characteristics that lead to a longer convergence time, by keeping degassing rates low, can also delay the beginning of degassing entirely: a high reference viscosity or low heat production rate. In addition, a low initial mantle temperature also delays degassing, as the mantle must heat up before it can melt in this case. As a result, convergence age shows some dependence on  $T_{\text{init}}$ , with lower  $T_{\text{init}}$  leading to larger convergence ages (Figure 3C). However, convergence time shows no discernible dependence on  $T_{\text{init}}$  (Figure 4C), because once degassing has begun, the influence of the initial mantle temperature has already been lost. The rate of degassing after this point will solely depend on the vigor of convection, which is controlled by the mantle viscosity and heating power available to drive convection. The convergence time depends modestly on the total carbon budget, as described above, but the convergence age does not (Figure 3D). The planet age when degassing begins does not depend on  $C_{\text{tot}}$ , as long as there are at least some interior volatiles available to degas, because it only depends on how long it takes for the mantle to heat up enough to melt (neglecting any possible dependence of the mantle solidus on mantle C content). The way a higher carbon budget helps enhance degassing rates once volcanism has begun is swamped out by the time it takes for volcanism to begin when looking convergence age.

Overall,  $\approx 90\%$  of our models produce climate convergence ages that are greater than the age of the AU Mic system. Habitable terrestrial exoplanets in systems of similar age to AU Mic are therefore highly likely to have atmospheres that are still in some state of transition from their initial conditions, and therefore inform the range of initial atmospheric conditions on terrestrial exoplanets. Models that produce convergence ages  $< 20$  Myrs are preferentially those with low reference viscosities  $< 10^{20}$  Pa s, and high initial mantle temperatures  $> 1800$  K (Figure 5). Very young convergence ages are seen for the full range of initial radiogenic heat production rates we explored, so there is no strong connection between heat budget and producing convergence ages  $< 20$  Myrs. For a very young convergence age, it is important for extensive volcanism to begin very early in a planet’s history, and this is more readily accomplished through an initially hot mantle than through high rates of heat production. Even with a high internal heating rate, there would still be a significant time lag before volcanism can begin if the initial mantle temperature is low. Consistent with our other results, neither the total C

budget nor the parameters for weathering exert a significant control on producing very short convergence ages. In sum, only planets with high initial mantle temperatures and low reference viscosities would be expected to have lost the influence of their initial atmospheric state by the  $\approx 20$  Myr age of AU Mic, absent other factors, such as atmospheric escape, we discuss next.

### 3.3. Additional Atmosphere Evolution Factors

Our models of outgassing, the carbonate-silicate cycle, and climate evolution ignore stellar evolution, when in reality stars are typically rapidly evolving during this early phase of their lifetimes. In the case of AU Mic, luminosity is decreasing as the star evolves towards the main sequence. This shift in luminosity changes the position of the HZ, but not by so much that planets can not stay within the HZ throughout the entire evolution. We therefore first discuss how changing solar luminosity would change our model results for a planet that always remains in the HZ. More extreme evolution, where planets may start in a runaway greenhouse state before ending up in the HZ after the star reaches the main sequence, will be discussed later. For a planet that is always in the HZ during the star’s pre-main sequence phase, decreasing luminosity would lead to a cooling climate. The carbonate-silicate cycle on such a planet would then respond by acting to boost the atmospheric  $\text{CO}_2$  content, as a result of a temporary slowdown in weathering rates caused by the cooling climate. A background secular trend that leads to climate cooling, and hence a buildup of atmospheric  $\text{CO}_2$  through the carbonate-silicate cycle, would act to increase the climate convergence times and ages we presented in Section 3.2, because it would require even more  $\text{CO}_2$  to be outgassed from the mantle in the initially cold climate state, before initial conditions are erased.

For increasing stellar luminosity, the effect runs the other way. Higher luminosity favors less  $\text{CO}_2$  in the atmosphere due to carbonate-silicate cycle feedbacks. Less  $\text{CO}_2$  from the interior needs to be outgassed to warm an initially cool climate, and therefore climate convergence ages and times would be shorter. These effects can of course be superimposed in the same system, as the star’s luminosity decreases during pre-main sequence evolution, and then increases when it reaches the main sequence. Given the timescales of stellar evolution, low mass stars would favor longer preservation of initial climate states, while high mass stars would favor these states being erased more quickly, as long as the planet remains in the HZ the whole time and escape rates are low enough for the atmosphere to be retained.

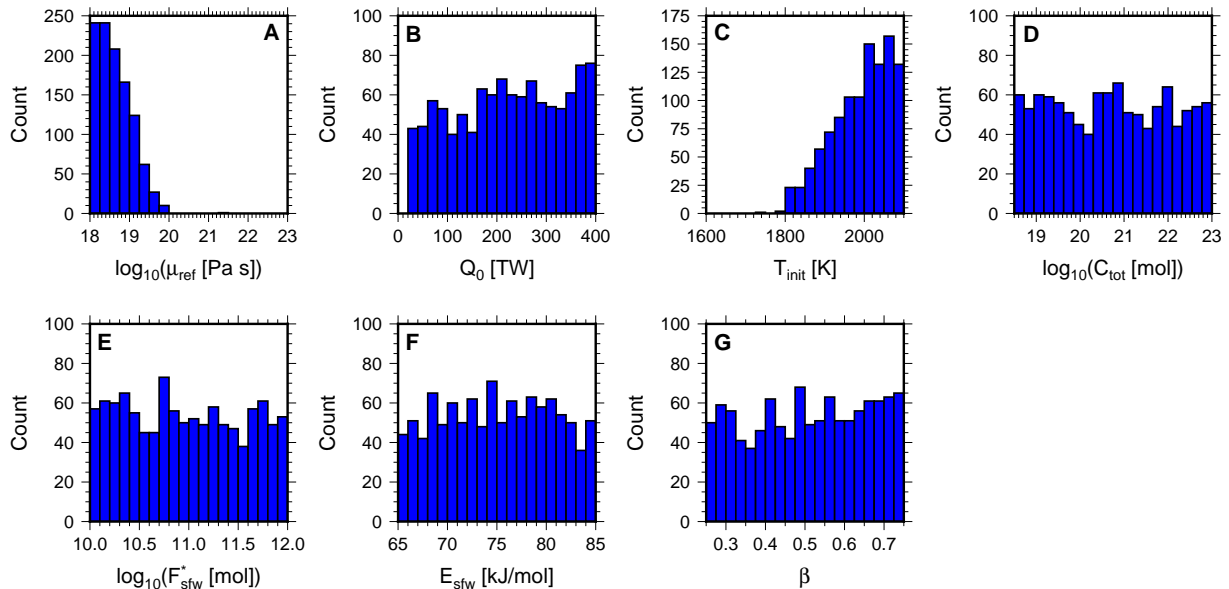


**Figure 5.** Histograms of model parameters for all models that produce climate convergence ages less than 20 Myrs, or approximately the age of the AU Mic system. Shown are distributions of mantle reference viscosity (A), initial heat production rate (B), initial mantle temperature (C), total carbon budget (D), reference seafloor weathering rate (E), activation energy for seafloor weathering (F), and dependence parameter of seafloor weathering on extrusive volcanism rate (G).

M-dwarf stars, especially the lowest mass M-dwarf stars, present a more extreme case, as they remain in a superluminous state during their early life for substantially longer than G-dwarfs, like the Sun (Luger & Barnes 2015). In such systems, the HZ boundaries can shift significantly, such that any planets in the HZ when the star reaches the main sequence will have been in a runaway greenhouse state during the pre-main sequence phase. In a runaway greenhouse climate, the lack of liquid water will largely eliminate silicate weathering, meaning all outgassed  $\text{CO}_2$  will remain in the atmosphere. In addition, rapid escape of both H and heavier species is likely (e.g. Ramirez & Kaltenegger 2014; Luger & Barnes 2015). Such rapid escape could quickly remove both any initial atmosphere left after magma ocean solidification, and any atmosphere outgassed by subsequent volcanism. Young planets in such a situation may still show an atmosphere in a transitional phase, but in this case a phase where rapid escape is depleting the atmosphere. If enough volatiles remain in the planetary interior after the star settles on to the main sequence, an atmosphere may be able to re-form by volcanic outgassing.

To quantify how atmospheric loss processes, either driven by hydrodynamic escape or non-thermal erosion, influence our  $\text{CO}_2$  outgassing and atmosphere evolution model results, we added a constant atmospheric loss rate to our models and varied this loss rate over a wide range (Figure 6 & 7). We ran sets of models individually varying the parameters found to influence climate conver-

gence age the most: mantle reference viscosity, initial internal heating rate, total carbon budget, and initial mantle temperature. Our thermal evolution models are tracking  $\text{CO}_2$  outgassing from the interior, so we assume a  $\text{CO}_2$  dominated atmosphere. Our imposed atmospheric loss rates are therefore rates of  $\text{CO}_2$  loss in  $\text{mol}\cdot\text{s}^{-1}$ .

At low atmospheric loss rates, the atmosphere is retained for at least 10 Gyrs (the ending time of our models), even though volcanism and degassing ends far earlier (Figure 6). The latest that volcanism lasts in any of our models shown in Figure 6 is  $\approx 4.5$  Gyrs. After degassing has ended, the atmosphere is simply lost at the imposed loss rate, until it is entirely depleted. Atmospheric retention time therefore scales inversely with loss rate. As a result, there is a threshold loss rate where the atmosphere can not be retained for 10 Gyrs or longer, and beyond this threshold the planet age where the atmosphere is totally lost decreases linearly with increasing loss rate. The behavior changes then when loss rates are high enough to entirely remove the atmosphere before degassing has ceased. Total atmospheric loss can happen while degassing is still active when the loss rate exceeds the degassing rate; in this case the existing atmosphere can be lost and degassing is unable to replenish the atmosphere. All degassed volatiles are rapidly lost to space. Degassing rate decreases over time as the planet cools, before falling to zero when volcanism stops. As a result, large atmospheric loss rates are needed to push the age when the atmosphere is lost further back



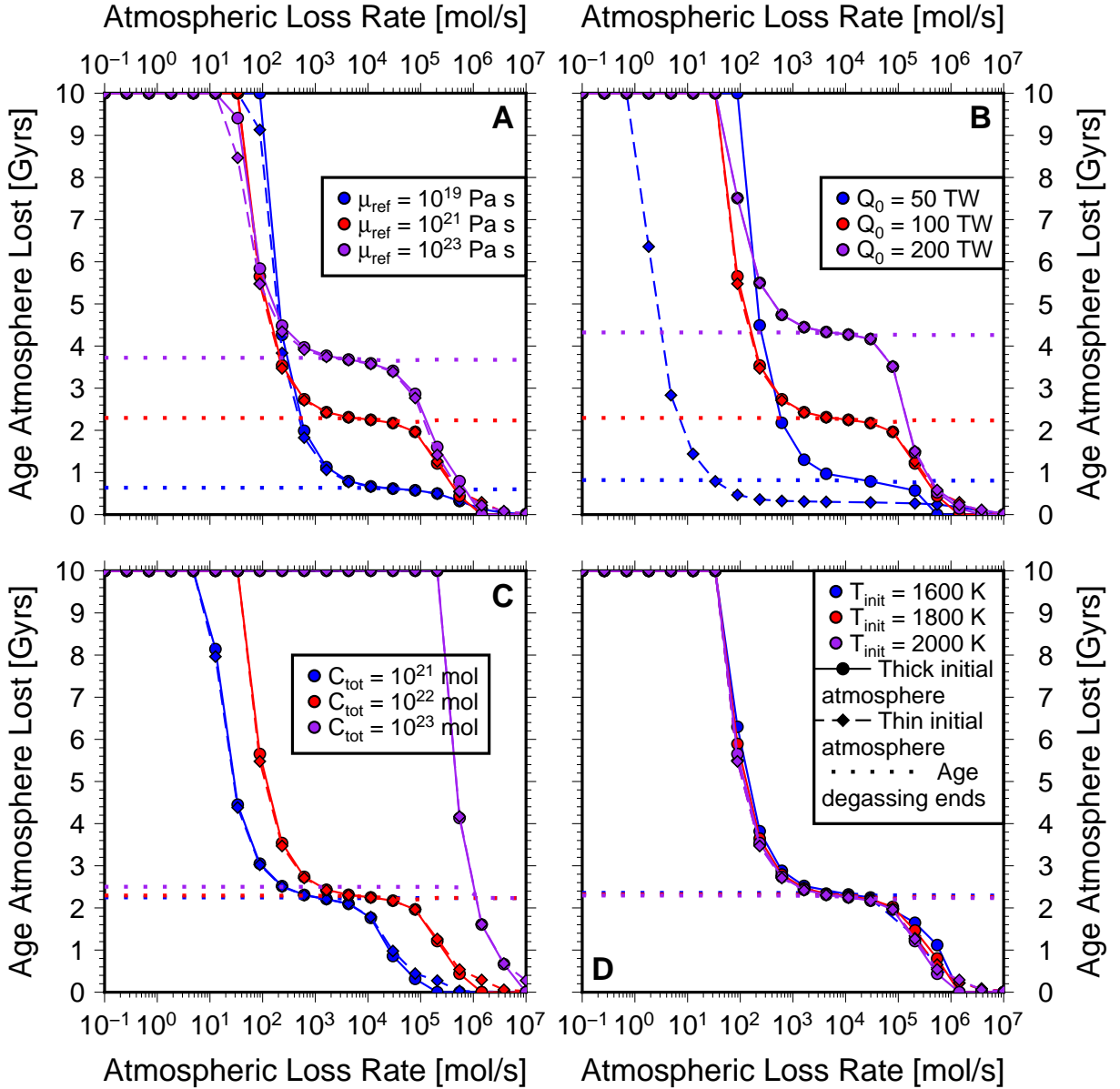


**Figure 6.** Planet age when the atmosphere is completely lost as a function of an imposed, constant atmospheric loss rate for varying mantle reference viscosity,  $\mu_{\text{ref}}$  (A), initial heat production rate,  $Q_0$  (B), mantle carbon budget,  $C_{\text{tot}}$  (C), and initial mantle temperature,  $T_{\text{init}}$  (D). All models assume  $F_{\text{sfw}}^* = 5 \times 10^{11} \text{ mol}\cdot\text{yr}^{-1}$ ,  $E_{\text{sfw}} = 75 \text{ kJ}\cdot\text{mol}^{-1}$ , and  $\beta = 0.5$ . Unless otherwise specified, models also assume  $\mu_{\text{ref}} = 10^{21} \text{ Pa}\cdot\text{s}$ ,  $Q_0 = 100 \text{ TW}$ ,  $C_{\text{tot}} = 10^{22} \text{ mol}$ , and  $T_{\text{init}} = 2000 \text{ K}$ . Model results are color coded based on the legends in each panel. Circles connected by solid lines are used for models started with a  $\text{CO}_2$ -rich initial atmosphere, and diamonds connected by dashed lines denote models with an initially  $\text{CO}_2$ -poor atmosphere. In many models sets there is little difference between the two initial conditions, so symbols lie on top of each other. Dotted lines show the age when interior degassing stops, color coded based on the legend for each panel. Models are run for 10 Gyrs, so models where an atmosphere is retained after 10 Gyrs are considered to have not lost their atmospheres.

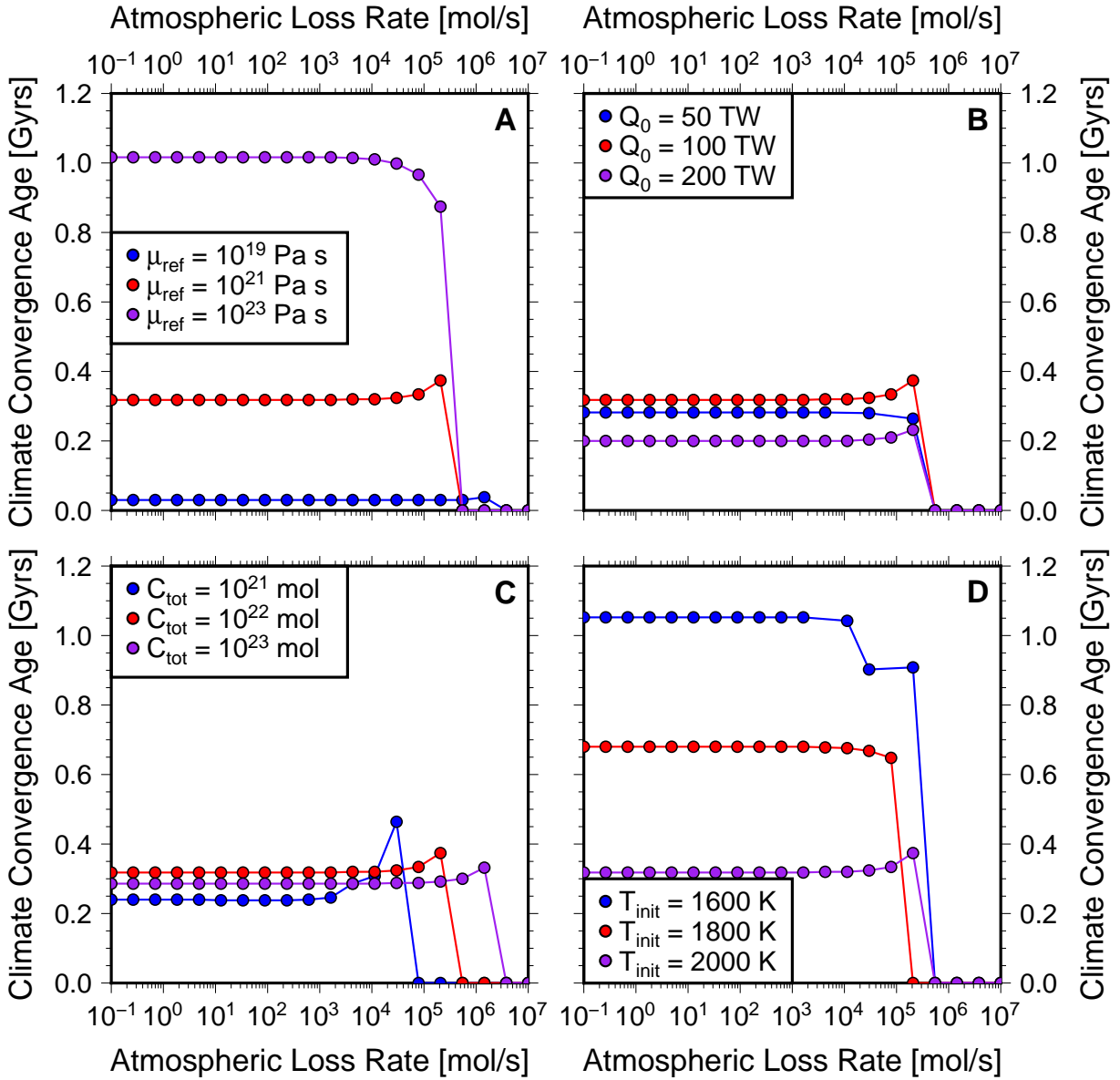


**Figure 7.** Climate convergence age as a function of an imposed, constant atmospheric loss rate for varying mantle reference viscosity,  $\mu_{\text{ref}}$  (A), initial heat production rate,  $Q_0$  (B), mantle carbon budget,  $C_{\text{tot}}$  (C), and initial mantle temperature,  $T_{\text{init}}$  (D). Other model parameters are the same as listed in the caption to Figure 6. Climate convergence age drops to zero when atmospheric loss is rapid enough to prevent any appreciable atmosphere from forming.

in time, to younger planet ages. Finally, the planet age when the atmosphere is lost drops towards zero when the loss rate exceeds even the peak degassing rate the planet experiences during its evolution. For loss rates this high the planet can effectively never form an atmosphere; anything degassed from the interior is rapidly lost to space.

The planet age where degassing ends is a function of mantle reference viscosity and initial heat budget (e.g. [Foley & Smye 2018](#)), leading to a corresponding change in the age where the atmosphere is lost. For atmospheric loss rates high enough to cause total atmosphere loss before degassing ends, but low enough to still allow an atmosphere to form, higher reference viscosities and higher initial heat production rates lead to longer retention of an atmosphere, because these effects prolong volcanism and degassing (Figure 6A & B). When the mantle carbon budget is increased, interior degassing rates are higher and a thicker atmosphere can form. As a result, the larger the carbon budget, the longer the atmosphere can be retained for a given loss rate (Figure 6C). Initial mantle temperature does not significantly influence rates of degassing over time, or when degassing ends, so it does not significantly influence the planet age where the atmosphere is lost. Finally, in most cases the initial atmospheric state does not affect the age when the atmosphere is lost. The one exception is the case with low initial heat production ( $Q_0 = 50$  TW, Figure 6B). In this case degassing rates are low and end early in the planet’s lifetime, after less than 1 Gyr. As a result, the initially CO<sub>2</sub>-poor atmosphere always stays thinner than the initially CO<sub>2</sub>-rich atmosphere, and hence is lost more quickly. Furthermore, as explained above, with initial heating rates this low planets with larger reference viscosities would not experience outgassing at all, especially with low initial mantle temperatures.

When atmospheric loss rates are high enough that the planet essentially never forms an atmosphere, or any primordial atmosphere is lost on a timescale of less than  $10^6 - 10^7$  yrs, then the issue of how long it takes two initially different climate states to converge is no longer relevant. The atmosphere is rapidly lost and observers would find a barren rock world. However, at lower loss rates that still allow an atmosphere to form, atmospheric loss could potentially influence the climate convergence ages and times presented in Section 3.2. On the contrary, we find that the climate convergence age is not strongly influenced by atmospheric loss, for loss rates low enough to allow an atmosphere to form (Figure 7). There is some effect for loss rates approaching the transition point where loss processes would prevent atmosphere formation entirely. The climate convergence age

can either decrease or increase by  $\sim 10 - 100$  Myrs depending on whether atmospheric loss acts more to remove an initially thick atmosphere or slow the buildup of an atmosphere by degassing when starting with an initially thin atmosphere. However, the largest effects of atmospheric loss on climate convergence age are seen for planets where the convergence age is already long,  $\sim 0.1 - 1$  Gyrs. For these planets, the effects of atmospheric loss are not sufficient to drive the convergence age below the age of the AU Mic system, except in the case of rates high enough to entirely remove the atmosphere.

Hydrodynamic escape driven by stellar extreme ultraviolet radiation is likely the dominant loss process for very young terrestrial planets (e.g. [Ramirez & Kaltenegger 2014](#); [Luger & Barnes 2015](#)). Stellar extreme ultraviolet fluxes,  $S_{EUV}$ , can be well fit with simple parameterizations based on stellar type (e.g. [Ribas et al. 2005](#)).  $S_{EUV}$  fluxes decrease over time, so rates of hydrodynamic escape will decline as well. Thus, in addition to constraining the atmospheric loss rates planets around young stars might experience, the duration of these high loss rates is also critical. Rapid early escape could remove any primordial atmosphere and prevent buildup of an outgassed atmosphere, but as these escape rates decline continued volcanism could then eventually produce a secondary atmosphere. Moreover, determining the escape rate a particular planet would experience is challenging, as this requires knowledge of the mixing ratios of the gases making up the atmosphere as a function of height. If hydrogen is abundant in the upper atmosphere, then escape is energy limited, which represents the upper bound on escape rates. Rapid hydrogen escape can also drag away heavier species, such as O or CO<sub>2</sub>. However, if the H mixing ratio is low, escape will be diffusion limited and much slower. Determining mixing ratios of different atmospheric species is beyond the scope of our simple outgassing models, but we can use previous studies on water loss as a first order guide.

[Ramirez & Kaltenegger \(2014\)](#) & [Luger & Barnes \(2015\)](#) show that H escape is rapid for planets in the main sequence habitable zone around low mass M-dwarf stars, due to the long pre-main sequence phase for these stars and the close-in main sequence habitable zone. The resulting flows of escaping H driven by high  $S_{EUV}$  fluxes are also capable of dragging heavier species, included CO<sub>2</sub>, with them. [Ramirez & Kaltenegger \(2014\)](#) find that the equivalent of  $\approx 200 - 4000$  times the molar quantity of H stored in Earth’s oceans can be lost for planets around the smallest M8 stars over the course of their  $\sim 1$  Gyr long pre-main sequence phase. This

corresponds to loss rates of  $\sim 10^8 - 10^{10}$  mol-s $^{-1}$  of H $_2$ . Such rapidly escaping H would also drag away substantial quantities of CO $_2$ , though with CO $_2$  escaping rates of H escape would be lower. Still, the lowest mass M dwarf stars can likely have nearly their entire volatile abundances stripped away by pre-main sequence  $S_{\text{EUV}}$  fluxes. Even continued volcanism after the star reaches the main sequence may not be able to replenish the atmosphere, as rapid early outgassing when the interior is hot can deplete the mantle of volatiles within  $\sim 1$  Gyr in our models.

Rather than being in a state of transition where the carbonate-silicate cycle is acting to bring the initial climate into an approximate steady-state between weathering and outgassing fluxes, planets around low mass M-dwarfs may instead have their volatiles entirely stripped. Observations of such planets in young systems are thus more likely to show runaway greenhouse climates and atmospheres being rapidly removed. Even if such planets are able to re-form an atmosphere after their host star reaches the main sequence, the initial atmospheric state after planet formation and any potential magma ocean solidification will have been lost. Planets re-forming their atmospheres will all be starting from similar states: essentially barren rocky worlds replenishing the atmosphere with volcanic gases.

More massive stars, including M1 stars and FGK stars, are more likely to retain atmospheres. Escape rates during these systems' early evolution can still be large, e.g.  $\sim 10^6 - 10^8$  mol-s $^{-1}$  of H $_2$  for planets around M1 stars, which can lose 0.5-25 Earth ocean masses of H $_2$  over  $\sim 200$  Myrs according to Ramirez & Kaltenegger (2014). However, these rapid escape rates are short lived, and the timespan of rapid escape shrinks as stellar mass increases. As a result, volatiles can still be retained after the star reaches the main sequence. We expect that water and CO $_2$  can therefore be retained around M1 stars and stars more massive than this. For M1 stars, early atmospheric escape may still be fast enough, and persist long enough, to remove an initially thick, CO $_2$ -rich atmosphere formed by outgassing from a magma ocean. In this case climate convergence may happen sooner than our models in Figures 3 & 4 indicate. Planets around young ( $< 100$  Myr old) M1 stars may have thin atmospheres due to atmospheric loss regardless of their initial atmospheric state. A more substantial atmosphere could then form after the star reaches the main sequence and escape rates fall. AU Mic itself is an M1 star, so it falls near this transition point where planets around stars less massive are likely to have initial atmospheric states erased very rapidly by escape, while planets in the HZ around more massive stars are likely

to retain their initial atmospheres and have their early climate evolution governed by the carbonate-silicate cycle feedbacks modeled in Section 3.2.

Our geophysical models assume that the planet has fully solidified from its initial magma ocean phase. This process of magma ocean solidification occurs over Myr timescales and is limited by the rate of heat loss at the top of the atmosphere to space. This heat loss to space must exceed the incident stellar radiation from the host-star then, for the magma ocean to cool and solidify. Hamano et al. (2013) modeled these competing effects for rocky planets and found that the lifetime of the magma ocean is dependent on a planet's orbital distance, which sets the incident radiation flux, and the rate of water loss at the top of the atmosphere due to hydrodynamic escape. Their models find that magma oceans can last from a few Myr for planet's within the HZ of a Sun-like star, to  $\sim 10^2$  Myr for those interior to it. This is independent of any tidal heating that may be present, which can potentially expand the magma ocean lifetime even further (Driscoll & Barnes 2015). At only  $\sim 20$  Myr old, any rocky exoplanets orbiting AU Mic may potentially still be in the magma ocean phase of planetary evolution. Detection of SO $_2$  or alkali-bearing species NaOH and KOH via atmospheric transmission spectroscopy may hint at active volcanism on these planets (Kaltenegger et al. 2010; Schaefer et al. 2012). These atmospheric species, however, do not reveal whether this volcanism is from traditional surface melting or directly from the magma ocean. More work is needed to understand how we can truly detect the presence of a magma ocean, however, young planetary systems, such as AU Mic, provide us with an excellent laboratory for understanding this critical part of planetary evolution.

## 4. ORBITAL DYNAMICS

### 4.1. Dynamics of the Known Planets

The orbital dynamics of young planetary systems play a key role in determining the long-term architecture of those systems. These early dynamical effects include interactions with the debris disk and other planets (Raymond et al. 2012; de Sousa et al. 2020) and close stellar encounters in cluster environments (Spurzem et al. 2009; Kane & Deveny 2018; van Elteren et al. 2019). Here we explore the dynamics of the two known planets in the system, adopting the orbital parameters provided by Cale et al. (2021) (see Section 2). We follow the methodology of Kane (2019); Kane et al. (2021), which uses the Mercury Integrator Package (Chambers 1999) with a hybrid symplectic/Bulirsch-Stoer integrator with a Jacobi coor-

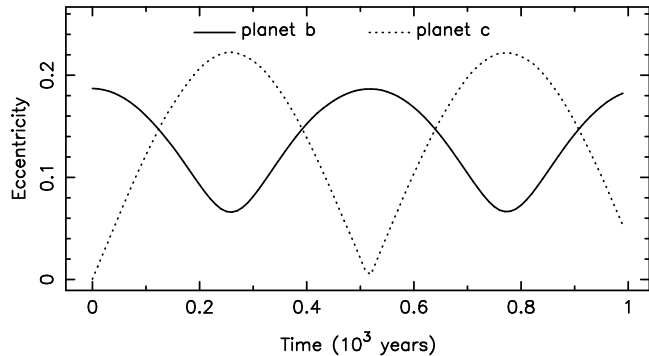


**Figure 8.** Orbital eccentricity as a function of time for the known planets, where planet b and planet c are shown as solid and dotted lines, respectively. The planets are long-term stable, but exchange significant angular momentum through oscillating eccentricities with a period of  $\sim 520$  yrs.

dinate system (Wisdom & Holman 1991; Wisdom 2006). Given the 8.46 day orbital period of the inner planet, we adopted a time resolution of 0.1 days to ensure sufficient accuracy during times of closest planet-planet interactions, as recommended by Duncan et al. (1998).

A suite of dynamical simulations was carried out that explored the long-term stability of the system for a range of orbital parameters within the measured uncertainties. The total duration of the simulations were  $10^8$  yrs, equivalent to  $\sim 2 \times 10^9$  orbits of planet c. These were all found to be stable over the full simulation durations. However, the disparity between the measured orbital eccentricities of the planets creates a high-frequency exchange of angular momentum. This exchange is visualized in Figure 8, which shows the eccentricity evolution of the planets over a period of  $10^3$  yrs. The period of the eccentricity variations is  $\sim 520$  yrs, consistent with the findings of previous investigations of the time-dependent dynamical effects of non-zero eccentricities (Gladman 1993; Chambers et al. 1996; Hadden & Lithwick 2018). Such eccentricity oscillations also have the potential to reduce the stability potential of other planets within the system, including terrestrial planets within the HZ.

#### 4.2. Stability Within the Habitable Zone

System orbital dynamics, such as those described in Section 4.1, can also have a dramatic effect on planets within the HZ, including their long-term stability (Georgakarakos et al. 2018; Kane et al. 2020c) and climate evolution (Way & Georgakarakos 2017; Kane et al. 2020d). Considering the evolution of the HZ described in Section 3.1, we performed a suite of dynamical simulations that tested the long-term stability of an Earth-mass planet in initial circular orbits with semi-major axes in the range 0.15–0.70 AU in steps of 0.005 AU. Each simulation was conducted for  $10^6$  years

with a time resolution of 0.1 days, as described in Section 4.1. The outcome of each simulation was assessed based on whether the injected Earth-mass planet survived or was lost, either by ejection from the system or lost to the gravitational well of the host star.

The results of the complete set of simulations are shown in Figure 9, where the simulation survival on the vertical axis refers to the percentage of the simulation for which the injected planet survived. The light green and dark green areas correspond to the CHZ and OHZ regions at the present epoch, respectively, equivalent to those shown in Figure 1. The vertical dashed lines represent the OHZ boundaries at a stellar age of 200 Myrs, based on the predicted stellar parameters described in Section 3.1 and the HZ boundaries shown in Figure 2. The simulations demonstrate that, although a terrestrial planet is able to retain orbital stability throughout the present HZ, such a planet can experience severe orbital instability near the inner edge of the main sequence HZ indicated by the vertical dashed lines. Therefore, a terrestrial planet that is currently located in the inner half of the present epoch (pre-main sequence) HZ, will find itself in a long-term stable orbit in the outer half of the main sequence HZ after the pre-main sequence phase of the stellar evolution is complete.

Although terrestrial planetary orbits have long-term stable locations within the inner half of the main sequence HZ, many of these locations experience significant eccentricity oscillations due to angular momentum transfer from the inner planets (see Section 4.1). Figure 10 shows the eccentricity evolution for the two known planets (solid and dotted lines) and a simulated terrestrial planet (planet d) located at 0.23 AU from the host star (dashed line). This particular location for planet d places the planet at the very edge of instability, as shown in Figure 9. In this case, planet d experiences variations in eccentricity within the range 0.0–0.3, resulting in periods of highly variable insolation flux received by the planet. Variable eccentricity such as this is known to play a substantial role in the planetary climate evolution, which can be dampened depending on the volatile inventory and spin state of the planet (Barnes et al. 2013; Linsenmeier et al. 2015; Way & Georgakarakos 2017; Kane et al. 2021). In terms of the early atmospheric evolution described in Section 3.2, the variable star–planet separations during periods of high eccentricity will cause correspondingly variable rates of atmospheric loss. Additionally, highly eccentric orbital states will induce tidal heating within the planet which, in turn, will contribute to the energy budget required for sustained degassing processes (Barnes et al. 2009; Driscoll & Barnes 2015). Thus,

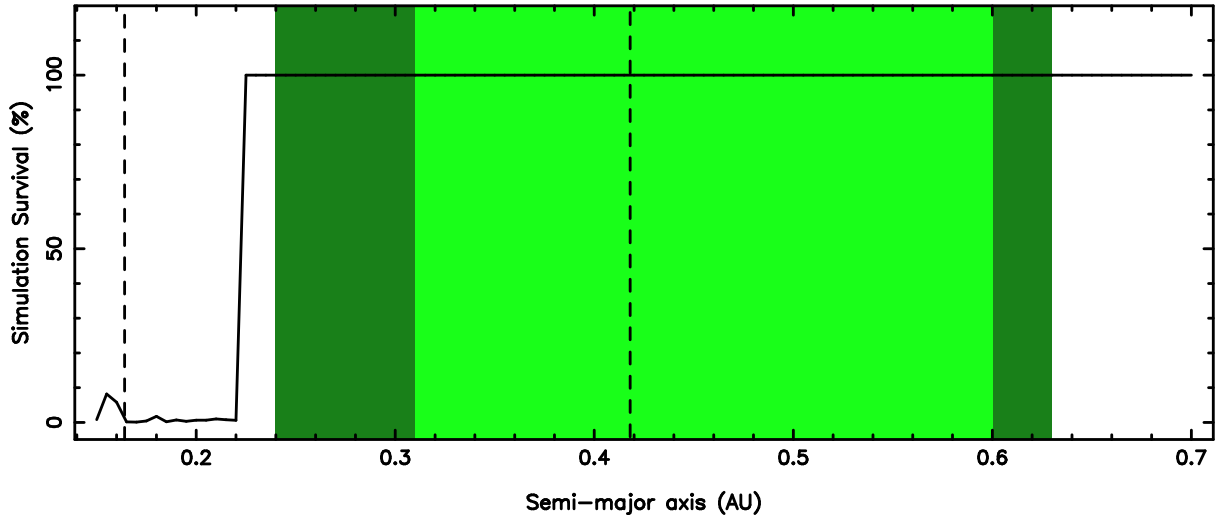


**Figure 9.** Plot of the dynamical simulation results for an Earth-mass planet injected in the semi-major axis range 0.15–0.70 AU. As for Figure 1, the light green and dark green areas represent the CHZ and OHZ regions at the present epoch, respectively. The vertical dashed lines represent the boundaries of the OHZ at a stellar age of 200 Myrs. The solid line shows the survival of the Earth-mass planet in terms of the percentage of the each simulation for which it remains in the system.

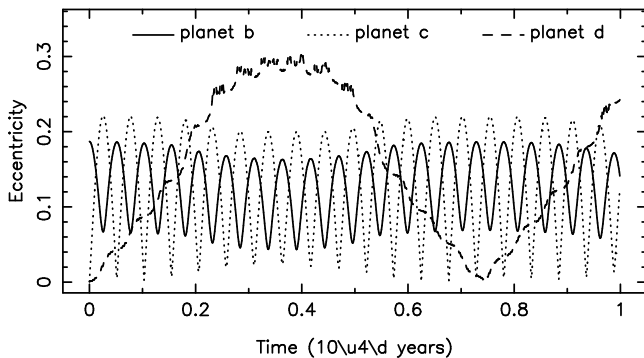


**Figure 10.** Eccentricity as a function of time for the known planets (solid and dotted lines) and a hypothetical terrestrial planet d with a semi-major axis of 0.23 AU (dashed line).

the combination of orbital state, atmospheric loss, and degassing rates creates a complex interaction between these processes that may serve to have a net positive or negative effect on long-term habitability, depending on factors such as the initial volatile inventory.

## 5. CONCLUSIONS

The early phase of both star and planet evolution are periods of rapid change for both classes of objects within the system. The changes occurring with the star result in a decreasing stellar luminosity, corresponding to a changing flux environment for the planets within the system. These changes, in turn, have consequences for the radiative balance of the new-formed planets, whose interior energy source will yet be substantial (Wetherill 1980; Kleine et al. 2002; Raymond et al. 2004). Furthermore, the dynamical state of young systems can be rel-

atively unstable and complex compared with their older counterparts, when much of the significant interactions and tidal dissipation will most likely have taken place. The AU mic system, being young, nearby, and containing two known transiting planets and a debris disk, provides an opportunity to conduct detailed studies of the early processes of planet formation and the convergence of potential planetary climates.

In this work, we have described a hypothetical terrestrial planet within the HZ of the AU Mic system. The evolutionary processes regarding the radiation environment and outgassing of the planet, described in Section 3, will play a critical role in the subsequent pathway of the overall planetary surface conditions (Hamano et al. 2013; Way & Del Genio 2020). Moreover, a non-zero eccentricity induced by interactions with the other planets in the system will add an additional time-dependent component to the radiation environment. An additional effect not considered in our outgassing model is that of atmospheric erosion, a process that is particularly efficient during the early stages of star and planet formation (Owen 2019; Rodríguez-Mozos & Moya 2019; Carolan et al. 2020). Continued observations of AU Mic are highly encouraged to further characterize the known planets and potentially detect additional planets in the system. An improved system architecture model would greatly aid in determining the viability of stable orbital locations within the system and how these would evolve through time. Further RV observations, such as those described by Cale et al. (2021), will potentially extend the sensitivity of the probed parameter space to longer peri-

ods and smaller masses. Additional *TESS* sectors that observe AU Mic will likewise refine the properties of the known planets as well as possibly reveal additional transiting planets within the system. Direct imaging of the star is lucrative due to its proximity, and has been used to study the debris disk at millimeter wavelengths (MacGregor et al. 2013), but will likely suffer from zodiacal dust contamination at optical wavelengths, inhibiting the detection of terrestrial planets within the HZ. Regardless, the AU Mic system is an incredibly important evolutionary case-study that will serve as a template for understanding how planets and their atmo-

spheres evolve during the crucial early stages of their lives.

#### ACKNOWLEDGEMENTS

This research has made use of the Habitable Zone Gallery at [hzgl.org](http://hzgl.org). The results reported herein benefited from collaborations and/or information exchange within NASA’s Nexus for Exoplanet System Science (NExSS) research coordination network sponsored by NASA’s Science Mission Directorate.

*Software:* Mercury (Chambers 1999)

#### REFERENCES

- Abbot, D. S., Cowan, N. B., & Ciesla, F. J. 2012, *ApJ*, 756, 178, doi: [10.1088/0004-637X/756/2/178](https://doi.org/10.1088/0004-637X/756/2/178)
- Baraffe, I., Chabrier, G., Allard, F., & Hauschildt, P. H. 2002, *A&A*, 382, 563, doi: [10.1051/0004-6361:20011638](https://doi.org/10.1051/0004-6361:20011638)
- Barnes, R., Jackson, B., Greenberg, R., & Raymond, S. N. 2009, *ApJL*, 700, L30, doi: [10.1088/0004-637X/700/1/L30](https://doi.org/10.1088/0004-637X/700/1/L30)
- Barnes, R., Mullins, K., Goldblatt, C., et al. 2013, *Astrobiology*, 13, 225, doi: [10.1089/ast.2012.0851](https://doi.org/10.1089/ast.2012.0851)
- Berner, R. A., & Caldeira, K. 1997, *Geology*, 25, 955, doi: [10.1130/0091-7613\(1997\)025\(0955:TNFMBA\)2.3.CO;2](https://doi.org/10.1130/0091-7613(1997)025(0955:TNFMBA)2.3.CO;2)
- Berner, R. A., Lasaga, A. C., & Garrels, R. M. 1983, *American Journal of Science*, 283, 641, doi: [10.2475/ajs.283.7.641](https://doi.org/10.2475/ajs.283.7.641)
- Bond, J. C., O’Brien, D. P., & LaRetta, D. S. 2010, *ApJ*, 715, 1050, doi: [10.1088/0004-637X/715/2/1050](https://doi.org/10.1088/0004-637X/715/2/1050)
- Cale, B., Plavchan, P., LeBrun, D., et al. 2019, *AJ*, 158, 170, doi: [10.3847/1538-3881/ab3b0f](https://doi.org/10.3847/1538-3881/ab3b0f)
- Cale, B., Reefe, M., Plavchan, P., et al. 2021, arXiv e-prints, arXiv:2109.13996. <https://arxiv.org/abs/2109.13996>
- Carolan, S., Vidotto, A. A., Plavchan, P., Villarreal D’Angelo, C., & Hazra, G. 2020, *MNRAS*, 498, L53, doi: [10.1093/mnras/slaal27](https://doi.org/10.1093/mnras/slaal27)
- Chambers, J. E. 1999, *MNRAS*, 304, 793, doi: [10.1046/j.1365-8711.1999.02379.x](https://doi.org/10.1046/j.1365-8711.1999.02379.x)
- Chambers, J. E., Wetherill, G. W., & Boss, A. P. 1996, *Icarus*, 119, 261, doi: [10.1006/icar.1996.0019](https://doi.org/10.1006/icar.1996.0019)
- Choi, J., Dotter, A., Conroy, C., et al. 2016, *ApJ*, 823, 102, doi: [10.3847/0004-637X/823/2/102](https://doi.org/10.3847/0004-637X/823/2/102)
- David, T. J., Petigura, E. A., Luger, R., et al. 2019a, *ApJL*, 885, L12, doi: [10.3847/2041-8213/ab4c99](https://doi.org/10.3847/2041-8213/ab4c99)
- David, T. J., Cody, A. M., Hedges, C. L., et al. 2019b, *AJ*, 158, 79, doi: [10.3847/1538-3881/ab290f](https://doi.org/10.3847/1538-3881/ab290f)
- Davies, D. W. 1980, *Icarus*, 42, 145, doi: [10.1016/0019-1035\(80\)90252-3](https://doi.org/10.1016/0019-1035(80)90252-3)
- de Sousa, R. R., Morbidelli, A., Raymond, S. N., et al. 2020, *Icarus*, 339, 113605, doi: [10.1016/j.icarus.2019.113605](https://doi.org/10.1016/j.icarus.2019.113605)
- Dong, C., Huang, Z., Lingam, M., et al. 2017, *ApJL*, 847, L4, doi: [10.3847/2041-8213/aa8a60](https://doi.org/10.3847/2041-8213/aa8a60)
- Dong, C., Jin, M., Lingam, M., et al. 2018, *Proceedings of the National Academy of Science*, 115, 260, doi: [10.1073/pnas.1708010115](https://doi.org/10.1073/pnas.1708010115)
- Dotter, A. 2016, *ApJS*, 222, 8, doi: [10.3847/0067-0049/222/1/8](https://doi.org/10.3847/0067-0049/222/1/8)
- Driscoll, P., & Bercovici, D. 2013, *Icarus*, 226, 1447, doi: [10.1016/j.icarus.2013.07.025](https://doi.org/10.1016/j.icarus.2013.07.025)
- Driscoll, P. E., & Barnes, R. 2015, *Astrobiology*, 15, 739, doi: [10.1089/ast.2015.1325](https://doi.org/10.1089/ast.2015.1325)
- Duncan, M. J., Levison, H. F., & Lee, M. H. 1998, *AJ*, 116, 2067, doi: [10.1086/300541](https://doi.org/10.1086/300541)
- Fogg, M. J., & Nelson, R. P. 2009, *A&A*, 498, 575, doi: [10.1051/0004-6361/200811305](https://doi.org/10.1051/0004-6361/200811305)
- Foley, B. J. 2015, *ApJ*, 812, 36, doi: [10.1088/0004-637X/812/1/36](https://doi.org/10.1088/0004-637X/812/1/36)
- . 2019, *ApJ*, 875, 72, doi: [10.3847/1538-4357/ab0f31](https://doi.org/10.3847/1538-4357/ab0f31)
- Foley, B. J., Bercovici, D., & Landuyt, W. 2012, *Earth and Planetary Science Letters*, 331, 281, doi: [10.1016/j.epsl.2012.03.028](https://doi.org/10.1016/j.epsl.2012.03.028)
- Foley, B. J., & Smye, A. J. 2018, *Astrobiology*, 18, 873, doi: [10.1089/ast.2017.1695](https://doi.org/10.1089/ast.2017.1695)
- Gaidos, E., Mann, A. W., Lépine, S., et al. 2014, *MNRAS*, 443, 2561, doi: [10.1093/mnras/stu1313](https://doi.org/10.1093/mnras/stu1313)
- Gaillard, F., & Scaillet, B. 2014, *Earth and Planetary Science Letters*, 403, 307, doi: [10.1016/j.epsl.2014.07.009](https://doi.org/10.1016/j.epsl.2014.07.009)
- Gallet, F., Charbonnel, C., Amard, L., et al. 2017, *A&A*, 597, A14, doi: [10.1051/0004-6361/201629034](https://doi.org/10.1051/0004-6361/201629034)
- Georgakarakos, N., Eggl, S., & Dobbs-Dixon, I. 2018, *ApJ*, 856, 155, doi: [10.3847/1538-4357/aaaf72](https://doi.org/10.3847/1538-4357/aaaf72)
- Gilbert, E. A., Barclay, T., Quintana, E. V., et al. 2021, arXiv e-prints, arXiv:2109.03924. <https://arxiv.org/abs/2109.03924>

- Gladman, B. 1993, *Icarus*, 106, 247, doi: [10.1006/icar.1993.1169](https://doi.org/10.1006/icar.1993.1169)
- Glaser, D. M., Hartnett, H. E., Desch, S. J., et al. 2020, *ApJ*, 893, 163, doi: [10.3847/1538-4357/ab822d](https://doi.org/10.3847/1538-4357/ab822d)
- Hadden, S., & Lithwick, Y. 2018, *AJ*, 156, 95, doi: [10.3847/1538-3881/aad32c](https://doi.org/10.3847/1538-3881/aad32c)
- Hamano, K., Abe, Y., & Genda, H. 2013, *Nature*, 497, 607, doi: [10.1038/nature12163](https://doi.org/10.1038/nature12163)
- Hayworth, B. P. C., & Foley, B. J. 2020, *ApJL*, 902, L10, doi: [10.3847/2041-8213/abb882](https://doi.org/10.3847/2041-8213/abb882)
- Howe, A. R., Adams, F. C., & Meyer, M. R. 2020, *ApJ*, 894, 130, doi: [10.3847/1538-4357/ab620c](https://doi.org/10.3847/1538-4357/ab620c)
- Johnstone, C. P., Khodachenko, M. L., Lüftinger, T., et al. 2019, *A&A*, 624, L10, doi: [10.1051/0004-6361/201935279](https://doi.org/10.1051/0004-6361/201935279)
- Kaltenegger, L., Henning, W. G., & Sasselov, D. D. 2010, *AJ*, 140, 1370, doi: [10.1088/0004-6256/140/5/1370](https://doi.org/10.1088/0004-6256/140/5/1370)
- Kane, S. R. 2014, *ApJ*, 782, 111, doi: [10.1088/0004-637X/782/2/111](https://doi.org/10.1088/0004-637X/782/2/111)
- . 2018, *ApJL*, 861, L21, doi: [10.3847/2041-8213/aad094](https://doi.org/10.3847/2041-8213/aad094)
- . 2019, *AJ*, 158, 72, doi: [10.3847/1538-3881/ab2a09](https://doi.org/10.3847/1538-3881/ab2a09)
- Kane, S. R., & Deveny, S. J. 2018, *ApJ*, 864, 115, doi: [10.3847/1538-4357/aad802](https://doi.org/10.3847/1538-4357/aad802)
- Kane, S. R., Fetherolf, T., & Hill, M. L. 2020a, *AJ*, 159, 176, doi: [10.3847/1538-3881/ab7818](https://doi.org/10.3847/1538-3881/ab7818)
- Kane, S. R., & Gelino, D. M. 2012, *PASP*, 124, 323, doi: [10.1086/665271](https://doi.org/10.1086/665271)
- Kane, S. R., Li, Z., Wolf, E. T., Ostberg, C., & Hill, M. L. 2021, *AJ*, 161, 31, doi: [10.3847/1538-3881/abcbfd](https://doi.org/10.3847/1538-3881/abcbfd)
- Kane, S. R., Meshkat, T., & Turnbull, M. C. 2018, *AJ*, 156, 267, doi: [10.3847/1538-3881/aae981](https://doi.org/10.3847/1538-3881/aae981)
- Kane, S. R., Roettenbacher, R. M., Unterborn, C. T., Foley, B. J., & Hill, M. L. 2020b, *The Planetary Science Journal*, 1, 36, doi: [10.3847/PSJ/abaab5](https://doi.org/10.3847/PSJ/abaab5)
- Kane, S. R., Turnbull, M. C., Fulton, B. J., et al. 2020c, *AJ*, 160, 81, doi: [10.3847/1538-3881/ab9ffe](https://doi.org/10.3847/1538-3881/ab9ffe)
- Kane, S. R., Vervoort, P., Horner, J., & Pozuelos, F. J. 2020d, *The Planetary Science Journal*, 1, 42, doi: [10.3847/PSJ/abae63](https://doi.org/10.3847/PSJ/abae63)
- Kane, S. R., Hill, M. L., Kasting, J. F., et al. 2016, *ApJ*, 830, 1, doi: [10.3847/0004-637X/830/1/1](https://doi.org/10.3847/0004-637X/830/1/1)
- Kasting, J. F., & Catling, D. 2003, *ARA&A*, 41, 429, doi: [10.1146/annurev.astro.41.071601.170049](https://doi.org/10.1146/annurev.astro.41.071601.170049)
- Kasting, J. F., Whitmire, D. P., & Reynolds, R. T. 1993, *Icarus*, 101, 108, doi: [10.1006/icar.1993.1010](https://doi.org/10.1006/icar.1993.1010)
- Kite, E. S., & Barnett, M. N. 2020, *Proceedings of the National Academy of Science*, 117, 18264. <https://arxiv.org/abs/2006.02589>
- Kleine, T., Münker, C., Mezger, K., & Palme, H. 2002, *Nature*, 418, 952, doi: [10.1038/nature00982](https://doi.org/10.1038/nature00982)
- Kochukhov, O., & Reiners, A. 2020, *ApJ*, 902, 43, doi: [10.3847/1538-4357/abb2a2](https://doi.org/10.3847/1538-4357/abb2a2)
- Kopparapu, R. K. 2013, *ApJ*, 767, L8, doi: [10.1088/2041-8205/767/1/L8](https://doi.org/10.1088/2041-8205/767/1/L8)
- Kopparapu, R. K., Ramirez, R. M., SchottelKotte, J., et al. 2014, *ApJ*, 787, L29, doi: [10.1088/2041-8205/787/2/L29](https://doi.org/10.1088/2041-8205/787/2/L29)
- Korenaga, J. 2010, *ApJL*, 725, L43, doi: [10.1088/2041-8205/725/1/L43](https://doi.org/10.1088/2041-8205/725/1/L43)
- Krissansen-Totton, J., & Catling, D. C. 2017, *Nature Communications*, 8, 15423, doi: [10.1038/ncomms15423](https://doi.org/10.1038/ncomms15423)
- Krissansen-Totton, J., Galloway, M. L., Wogan, N., Dhaliwal, J. K., & Fortney, J. J. 2021, *ApJ*, 913, 107, doi: [10.3847/1538-4357/abf560](https://doi.org/10.3847/1538-4357/abf560)
- Lalitha, S., Schmitt, J. H. M. M., & Dash, S. 2018, *MNRAS*, 477, 808, doi: [10.1093/mnras/sty732](https://doi.org/10.1093/mnras/sty732)
- Lammer, H., Kasting, J. F., Chassefière, E., et al. 2008, *SSRv*, 139, 399, doi: [10.1007/s11214-008-9413-5](https://doi.org/10.1007/s11214-008-9413-5)
- Lammer, H., Bredehöft, J. H., Coustenis, A., et al. 2009, *A&A Rv*, 17, 181, doi: [10.1007/s00159-009-0019-z](https://doi.org/10.1007/s00159-009-0019-z)
- Lenardic, A., & Crowley, J. W. 2012, *ApJ*, 755, 132, doi: [10.1088/0004-637X/755/2/132](https://doi.org/10.1088/0004-637X/755/2/132)
- Leto, G., Pagano, I., Linsky, J. L., Rodonò, M., & Umana, G. 2000, *A&A*, 359, 1035
- Levi, A., Sasselov, D., & Podolak, M. 2017, *ApJ*, 838, 24, doi: [10.3847/1538-4357/aa5cfe](https://doi.org/10.3847/1538-4357/aa5cfe)
- Linsenmeier, M., Pascale, S., & Lucarini, V. 2015, *Planet. Space Sci.*, 105, 43, doi: [10.1016/j.pss.2014.11.003](https://doi.org/10.1016/j.pss.2014.11.003)
- Luger, R., & Barnes, R. 2015, *Astrobiology*, 15, 119, doi: [10.1089/ast.2014.1231](https://doi.org/10.1089/ast.2014.1231)
- MacGregor, M. A., Wilner, D. J., Rosenfeld, K. A., et al. 2013, *ApJL*, 762, L21, doi: [10.1088/2041-8205/762/2/L21](https://doi.org/10.1088/2041-8205/762/2/L21)
- Magee, H. R. M., Güdel, M., Audard, M., & Mewe, R. 2003, *Advances in Space Research*, 32, 1149, doi: [10.1016/S0273-1177\(03\)00321-1](https://doi.org/10.1016/S0273-1177(03)00321-1)
- Mamajek, E. E., & Bell, C. P. M. 2014, *MNRAS*, 445, 2169, doi: [10.1093/mnras/stu1894](https://doi.org/10.1093/mnras/stu1894)
- Neves, V., Bonfils, X., Santos, N. C., et al. 2013, *A&A*, 551, A36, doi: [10.1051/0004-6361/201220574](https://doi.org/10.1051/0004-6361/201220574)
- Newton, E. R., Mann, A. W., Tofflemire, B. M., et al. 2019, *ApJL*, 880, L17, doi: [10.3847/2041-8213/ab2988](https://doi.org/10.3847/2041-8213/ab2988)
- Noack, L., & Breuer, D. 2014, *Planet. Space Sci.*, 98, 41, doi: [10.1016/j.pss.2013.06.020](https://doi.org/10.1016/j.pss.2013.06.020)
- O'Brien, D. P., Izidoro, A., Jacobson, S. A., Raymond, S. N., & Rubie, D. C. 2018, *SSRv*, 214, 47, doi: [10.1007/s11214-018-0475-8](https://doi.org/10.1007/s11214-018-0475-8)
- O'Neill, C., & Lenardic, A. 2007, *Geophys. Res. Lett.*, 34, L19204, doi: [10.1029/2007GL030598](https://doi.org/10.1029/2007GL030598)
- Oosterloo, M., Höning, D., Kamp, I. E. E., & van der Tak, F. F. S. 2021, *A&A*, 649, A15, doi: [10.1051/0004-6361/202039664](https://doi.org/10.1051/0004-6361/202039664)



- Owen, J. E. 2019, *Annual Review of Earth and Planetary Sciences*, 47, 67, doi: [10.1146/annurev-earth-053018-060246](https://doi.org/10.1146/annurev-earth-053018-060246)
- Paxton, B., Bildsten, L., Dotter, A., et al. 2011, *ApJS*, 192, 3, doi: [10.1088/0067-0049/192/1/3](https://doi.org/10.1088/0067-0049/192/1/3)
- Paxton, B., Cantiello, M., Arras, P., et al. 2013, *ApJS*, 208, 4, doi: [10.1088/0067-0049/208/1/4](https://doi.org/10.1088/0067-0049/208/1/4)
- Paxton, B., Marchant, P., Schwab, J., et al. 2015, *ApJS*, 220, 15, doi: [10.1088/0067-0049/220/1/15](https://doi.org/10.1088/0067-0049/220/1/15)
- Paxton, B., Schwab, J., Bauer, E. B., et al. 2018, *ApJS*, 234, 34, doi: [10.3847/1538-4365/aaa5a8](https://doi.org/10.3847/1538-4365/aaa5a8)
- Paxton, B., Smolec, R., Schwab, J., et al. 2019, *ApJS*, 243, 10, doi: [10.3847/1538-4365/ab2241](https://doi.org/10.3847/1538-4365/ab2241)
- Pepe, F., Mayor, M., Delabre, B., et al. 2000, in *Society of Photo-Optical Instrumentation Engineers (SPIE) Conference Series*, Vol. 4008, Proc. SPIE, ed. M. Iye & A. F. Moorwood, 582–592, doi: [10.1117/12.395516](https://doi.org/10.1117/12.395516)
- Plavchan, P., Barclay, T., Gagné, J., et al. 2020, *Nature*, 582, 497, doi: [10.1038/s41586-020-2400-z](https://doi.org/10.1038/s41586-020-2400-z)
- Ramirez, R. M., & Kaltenegger, L. 2014, *ApJL*, 797, L25, doi: [10.1088/2041-8205/797/2/L25](https://doi.org/10.1088/2041-8205/797/2/L25)
- Raymond, S. N., Mandell, A. M., & Sigurdsson, S. 2006, *Science*, 313, 1413, doi: [10.1126/science.1130461](https://doi.org/10.1126/science.1130461)
- Raymond, S. N., Quinn, T., & Lunine, J. I. 2004, *Icarus*, 168, 1, doi: [10.1016/j.icarus.2003.11.019](https://doi.org/10.1016/j.icarus.2003.11.019)
- . 2005, *Icarus*, 177, 256, doi: [10.1016/j.icarus.2005.03.008](https://doi.org/10.1016/j.icarus.2005.03.008)
- Raymond, S. N., Armitage, P. J., Moro-Martín, A., et al. 2012, *A&A*, 541, A11, doi: [10.1051/0004-6361/201117049](https://doi.org/10.1051/0004-6361/201117049)
- Ribas, I., Guinan, E. F., Güdel, M., & Audard, M. 2005, *ApJ*, 622, 680, doi: [10.1086/427977](https://doi.org/10.1086/427977)
- Ricker, G. R., Winn, J. N., Vanderspek, R., et al. 2015, *Journal of Astronomical Telescopes, Instruments, and Systems*, 1, 014003, doi: [10.1117/1.JATIS.1.1.014003](https://doi.org/10.1117/1.JATIS.1.1.014003)
- Rodríguez-Mozos, J. M., & Moya, A. 2019, *A&A*, 630, A52, doi: [10.1051/0004-6361/201935543](https://doi.org/10.1051/0004-6361/201935543)
- Roettenbacher, R. M., & Kane, S. R. 2017, *ApJ*, 851, 77, doi: [10.3847/1538-4357/aa991e](https://doi.org/10.3847/1538-4357/aa991e)
- Schaefer, L., Lodders, K., & Fegley, B. 2012, *ApJ*, 755, 41, doi: [10.1088/0004-637X/755/1/41](https://doi.org/10.1088/0004-637X/755/1/41)
- Schlichting, H. E., Sari, R., & Yalinewich, A. 2015, *Icarus*, 247, 81, doi: [10.1016/j.icarus.2014.09.053](https://doi.org/10.1016/j.icarus.2014.09.053)
- Spurzem, R., Giersz, M., Hogg, D. C., & Lin, D. N. C. 2009, *ApJ*, 697, 458, doi: [10.1088/0004-637X/697/1/458](https://doi.org/10.1088/0004-637X/697/1/458)
- Strubbe, L. E., & Chiang, E. I. 2006, *ApJ*, 648, 652, doi: [10.1086/505736](https://doi.org/10.1086/505736)
- Truitt, A., & Young, P. A. 2017, *ApJ*, 835, 87, doi: [10.3847/1538-4357/835/1/87](https://doi.org/10.3847/1538-4357/835/1/87)
- Truitt, A., Young, P. A., Spacek, A., Probst, L., & Dietrich, J. 2015, *ApJ*, 804, 145, doi: [10.1088/0004-637X/804/2/145](https://doi.org/10.1088/0004-637X/804/2/145)
- Tsikoudi, V., & Kellett, B. J. 2000, *MNRAS*, 319, 1147, doi: [10.1046/j.1365-8711.2000.03905.x](https://doi.org/10.1046/j.1365-8711.2000.03905.x)
- Underwood, D. R., Jones, B. W., & Sleep, P. N. 2003, *International Journal of Astrobiology*, 2, 289, doi: [10.1017/S1473550404001715](https://doi.org/10.1017/S1473550404001715)
- Valencia, D., O’Connell, R. J., & Sasselov, D. D. 2007, *ApJL*, 670, L45, doi: [10.1086/524012](https://doi.org/10.1086/524012)
- Valle, G., Dell’Omodarme, M., Prada Moroni, P. G., & Degl’Innocenti, S. 2014, *A&A*, 567, A133, doi: [10.1051/0004-6361/201323350](https://doi.org/10.1051/0004-6361/201323350)
- van Elteren, A., Portegies Zwart, S., Pelupessy, I., Cai, M. X., & McMillan, S. L. W. 2019, *A&A*, 624, A120, doi: [10.1051/0004-6361/201834641](https://doi.org/10.1051/0004-6361/201834641)
- van Heck, H. J., & Tackley, P. J. 2011, *Earth and Planetary Science Letters*, 310, 252, doi: [10.1016/j.epsl.2011.07.029](https://doi.org/10.1016/j.epsl.2011.07.029)
- Vogt, S. S., Allen, S. L., Bigelow, B. C., et al. 1994, *Society of Photo-Optical Instrumentation Engineers (SPIE) Conference Series*, Vol. 2198, HIREs: the high-resolution echelle spectrometer on the Keck 10-m Telescope (SPIE Press), 362, doi: [10.1117/12.176725](https://doi.org/10.1117/12.176725)
- Walker, J. C. G., Hays, P. B., & Kasting, J. F. 1981, *J. Geophys. Res.*, 86, 9776, doi: [10.1029/JC086iC10p09776](https://doi.org/10.1029/JC086iC10p09776)
- Way, M. J., & Del Genio, A. D. 2020, *Journal of Geophysical Research (Planets)*, 125, e06276, doi: [10.1029/2019JE006276](https://doi.org/10.1029/2019JE006276)
- Way, M. J., & Georgakarakos, N. 2017, *ApJ*, 835, L1, doi: [10.3847/2041-8213/835/1/L1](https://doi.org/10.3847/2041-8213/835/1/L1)
- Wetherill, G. W. 1980, *ARA&A*, 18, 77, doi: [10.1146/annurev.aa.18.090180.000453](https://doi.org/10.1146/annurev.aa.18.090180.000453)
- Wisdom, J. 2006, *AJ*, 131, 2294, doi: [10.1086/500829](https://doi.org/10.1086/500829)
- Wisdom, J., & Holman, M. 1991, *AJ*, 102, 1528, doi: [10.1086/115978](https://doi.org/10.1086/115978)
- Young, P. A., Liebst, K., & Pagano, M. 2012, *ApJL*, 755, L31, doi: [10.1088/2041-8205/755/2/L31](https://doi.org/10.1088/2041-8205/755/2/L31)
- Zendejas, J., Segura, A., & Raga, A. C. 2010, *Icarus*, 210, 539, doi: [10.1016/j.icarus.2010.07.013](https://doi.org/10.1016/j.icarus.2010.07.013)